NEAR-FIELD AND REGIONAL MODELING OF EXPLOSIONS AT THE DEGELEN TEST SITE

Jeffry L. Stevens,[1] Norton Rimer,[1] Heming Xu,[1] G. Eli Baker,[1] John R. Murphy,[1]
Gevorg G. Kocharyan[2] and Boris A. Ivanov[2]

Science Applications International Corporation,[1] Institute for the Dynamics of the Geospheres[2]

Sponsored by Defense Threat Reduction Agency

Contract No. DTRA01-00-C-0050

ABSTRACT

The objective of this research program is to improve the capability to predict the seismic source characteristics of underground explosions in rock. This is being accomplished by development of improved dynamic failure models that are constrained by a large unique data set of near-field waveforms and parametric data from both US tests and historic Soviet explosions at the Degelen Test Site. In addition, we are analyzing regional seismic data along a seismic line located north of the Degelen Test Site that recorded data at nine stations spaced approximately evenly from the test site to a distance of about 100 km. This project is a collaborative effort between SAIC and the Russian Institute for the Dynamics of the Geospheres (IDG).

IDG is in the process of digitizing data from 25 nuclear tests at Degelen. The complete data set consists of 81 near-field waveforms recorded underground at shot depth and 124 near-regional seismic records. Most seismic records include both a vertical and radial waveform. This data set provides a rare opportunity to observe and model the seismic wavefield of the explosions as they evolve from the near field of the explosion out to regional distances. To date, IDG has digitized 75 near-field waveforms and 97 seismic waveforms from 16 events having explosive yields ranging from 0.3 kT up to 125 kT. We are in the process of defining the optimum procedures to model these data. The goal is to develop material models that are consistent with the data and have a realistic physical basis. Work to date at SAIC has focused on implementation and testing of improved numerical modeling procedures and simulation of near-regional data. We are testing acoustic fluidization as a physical mechanism for strength reduction in nonlinear explosion simulations. Near regional data is being modeled using wave number integration. We are also comparing the Degelen data with similar data from the Piledriver and Hardhat Nevada Test Site (NTS) explosions in granitic rocks.

To more easily compare these data, we scaled all of the Degelen and NTS near-field particle velocity records to the same explosive yield. These data were then organized based on yield-scaled pulse widths and pulse shapes. The NTS events, the seven Degelen explosions with yields greater than 18 kT, and some of the lower yield events, gave records with positive and negative pulse widths that strongly suggest free-field ground motion. The records from a few of the other, lowest yield explosions had unusual shapes that indicated probable contamination by nearby fault or block motion. There is considerable variation among the pulse amplitudes and shapes of the free-field data. Some of this variation, particularly the consistent differences in pulse width, indicates some interesting and potentially important differences in physical mechanisms operating for subsets of explosions. Peak velocities at a given scaled range from the free-field events vary by a factor of 4, while positive pulse widths from Degelen vary by a factor of 3. Even the widest pulses from Degelen explosions, however, with one exception, are narrower than the pulse widths from the NTS events. Three of the higher yield explosions from Degelen, with yields of 125, 100, and 23.7 kT, form a "narrow pulse set" that were numerically simulated without the use of any strength reduction mechanism. The other four higher yield Degelen explosions, with yields from 19 to 78 kT, and some of the lower yield events, form a "wide pulse set", encompassing a gradation of pulse widths, that require the use of a gradation of strength reduction parameters in the numerical simulations. Simulation of the even wider pulses from the NTS explosions may be accomplished using different parameters in the same strength reduction model. The effects on pulse widths resulting from changes in Degelen site material properties due to earlier nearby explosions has yet to be quantified. The data set of near-field and regional waveforms will be delivered to the Center for Monitoring Research upon completion of this project.

OBJECTIVE

The main objective of this research program is to improve the capability to predict the seismic source characteristics of underground explosions in rock. This is being accomplished by development of improved dynamic failure models for hardrock that are constrained by a large unique data set of near-field waveforms and parametric data from both US tests and historic Soviet explosions at the Degelen Test Site. In addition, we are analyzing regional seismic data along a seismic line located north of the Degelen Test Site that recorded data at nine stations spaced approximately evenly from the test site to a distance of about 100 km. This project is a collaborative effort between SAIC and the Russian Institute for the Dynamics of the Geospheres (IDG).

RESEARCH ACCOMPLISHED

Introduction

Empirical and numerical models of explosion sources do a fairly good job of matching observed seismic signals, but the physical basis for the explosion source is still not well understood. In particular, numerical models of explosion sources developed using laboratory measurements of rock properties predict particle velocity pulse widths that are roughly a factor of 3-5 smaller than those observed near field in hardrock events such as Piledriver. The basic problem is that the strength of the rock measured in the laboratory is much larger than the apparent strength of the rock as determined from the near field ground motion.

A number of solutions to these problems have been proposed over the years, including the effective stress model (Rimer, *et al*, 1984), and various types of damage models. These models all have the characteristic that the material strength is reduced dynamically to a very low level when the rock fails. The effective stress model says that the weakness comes from water within the rock matrix, and that the broken rock in effect floats on water that is squeezed out of pores or fractures when the rock fails. Although there are questions about the realism of this physical model, it works fairly well to explain the near field waveforms. Figure 1 shows a comparison of the Piledriver waveforms with waveforms calculated using the effective stress model. The agreement is quite good, particularly at the closer two stations. Furthermore, when the Piledriver simulation was scaled to the appropriate yield and compared with other US explosions in granite (Hardhat and Shoal), agreement with the observed waveforms was also quite good (Stevens, *et al*, 1986).

Under a previous DTRA contract, SAIC worked together with the IDG and the University of Southern California (USC) to develop improved material models. IDG provided extensive pre- and post-shot measurements of material properties close to nuclear and chemical explosions. SAIC implemented the damage mechanics model for the growth and coalescence of cracks in brittle rocks under compressive loading which was developed by Prof. Charles Sammis of USC into our nonlinear finite difference codes and then used this model to simulate the observed explosion damage and a small set of near field waveforms provided by IDG. Since the Sammis damage model does not predict what happens to the rock after unstable brittle failure occurs, we introduced a friction law model post-failure. However, realistic values of friction did not provide enough strength reduction to match the near field data. To match the data, the coefficient of friction must be dropped to very low values (as low as 0.02) for rubbleized rock, but this again leaves the question of what physical mechanism could be responsible for these very low values and corresponding low strength. See Rimer *et al* (1999) for the results of this work.

A possible answer initially proposed by Melosh (1979) is “acoustic fluidization”. The physics behind this mechanism is that there is a complex dynamic acoustic wavefield that causes high frequency vibrations in the broken rock. These vibrations cause rapidly changing regions of high and low normal stress, and remove the frictional normal stress from parts of the rock as it moves. Consequently parts of the rock are not confined by the frictional stress and in effect have much lower strength. Acoustic fluidization has been used to explain other phenomena such as landslides and craters (Melosh and Ivanov, 1999), which have been similarly difficult to explain because of anomalously low apparent friction.

Analyses of Degelen Near Field and Near Regional Seismic Data

The numerical modeling component of this project is being constrained by a much better data set than has been available in the past, including near field waveforms from both US nuclear tests and the testing program of the

former Soviet Union. IDG has near field records from a number of nuclear explosions at the Degelen test site that are being digitized for this project. IDG will also be providing near source material properties measurements from these events. In addition, IDG has data from a seismic line located north of the Degelen test site that was maintained with consistent instrumentation for many years during the Soviet testing program. Figure 2 shows a map illustrating the location of the test sites and the seismic stations. The 9 seismic stations are spread out at approximately even intervals from the Degelen test site out to a distance of about 100 km. IDG is also digitizing seismic data from these stations for all of the events that have near field records. This provides a rare opportunity to observe and model the seismic wavefield of the explosions as they evolve from the near field of the explosion out to regional distances. The data that IDG has identified for digitization, and the data digitized as of this writing are listed in Table 1. Figure 3 shows waveforms from one of these explosions.

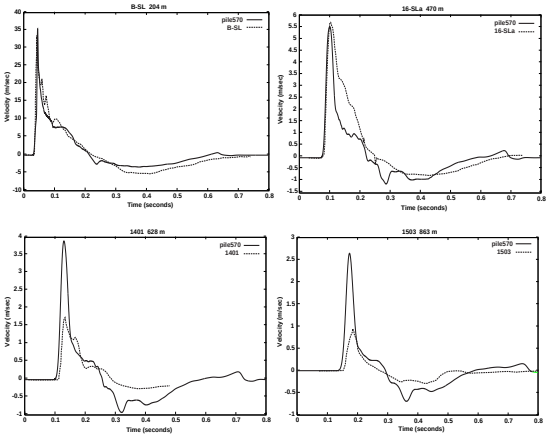

Figure 1. Particle velocity measurements at working point depth from Piledriver compared to numerical simulation pile570.

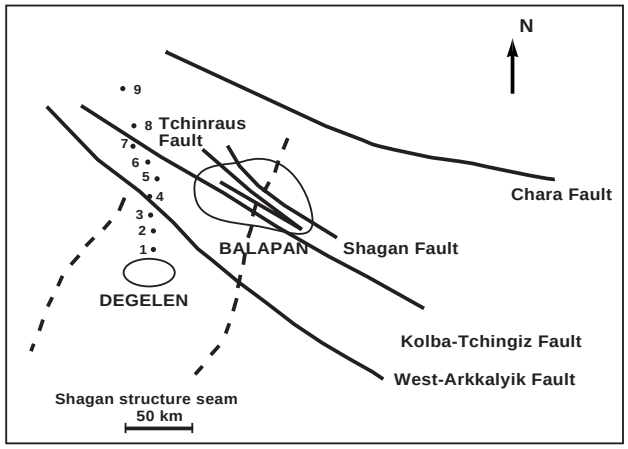

Figure 2. Map showing the locations of the former Soviet Degelen and Balapan test sites, faults, and seismic stations.

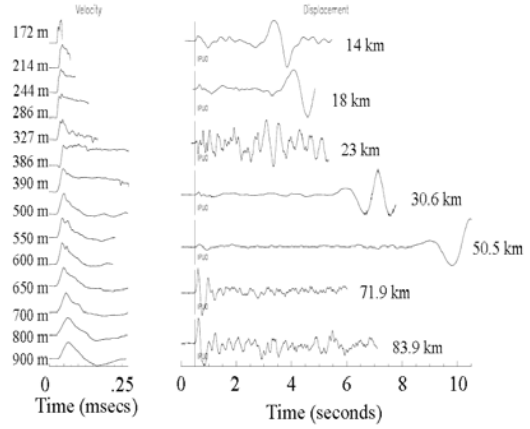

Figure 3. Near-field (left) and near regional seismic (right) waveforms from the 1987/07/17 event.

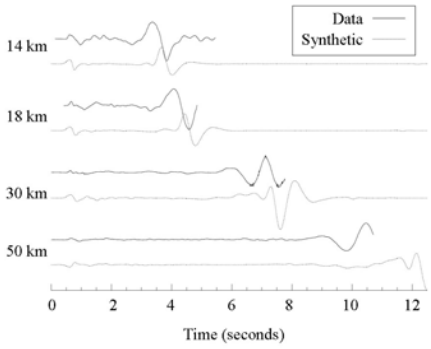

Figure 4. Synthetic and observed seismograms for the 1987/07/17 event. Synthetics were created using wavenumber integration and were low pass filtered at 2 Hz.

The near field records in Figure 3 show the evolution of the waveform from the nonlinear to linear regions. Unfortunately, the absolute times are not yet available for the records. The near regional records show the evolution of the waveform from 14 to 83 km. A strong Rg phase is present in several seismograms that persists to quite a long distance. Some of the records end before the start of the Rg phase and therefore do not show it. Figure 4 shows a comparison of synthetic and observed seismograms for three of the near regional waveforms from the 1987/07/17 event. The synthetic seismograms were constructed using wavenumber integration using the East Kazakh structure. The synthetic seismograms were low-pass filtered at 2 Hz. The persistence of Rg calls into question the explanation of Rg scattering as the source of Lg since that mechanism requires most of Rg to scatter into Lg within a few kilometers of the source.

Figure 5 shows a comparison between near-field peak particle velocity measurements from the Degelen explosions and from explosions at the US and French (Hoggar) granite sites. The solid curve gives peak velocities from the

Table 1. **Degelen events with near field and/or seismic records and waveforms digitized. Total number of records including multiples are shown in parentheses. Explosion yield, m_b , and depth of burial are shown.**

Date	Yield (kT)	m_b	Depth of Burial, (m)	No. of Near field records	Number Digitized	Distance Range, (m)	No. of Seismic Records	Number Digitized	Distance Range, (km)
1988/04/22	2.3	4.9	124	2	2	69-183	3	3 (11)	57-81
1988/11/23	19	5.4	204	4	3	280-475	9	9 (26)	14-83
1987/07/17	78	5.8	267	14	14	170-900	7	7 (23)	14.5-84
1987/10/16	1.1	4.6	82	4	4	55-132	8	8 (27)	4-64
1989/10/04	1.8	4.7	94	4	4 (5)	45-285	8	8 (25)	16-85
1981/07/17	9.3	5.16	146	3	3	115-310	8	8 (27)	15-80
1965/02/04	18/44	-	262	4	4	147-750	9	peaks	14-83
1964/05/16	23.7	5.6	253/ 262	4	4	150-600	9	peaks	13-79
1966/03/20	100	6.0	294/ 320	4	4	300-600	9	peaks	15-84
1966/02/13	125	6.1	297/ 343	4	4	350-600	9	peaks	14-79
1973/12/31	0.5	-	157	4	4(5)	110-230			
1974/12/16	3	4.8	126	4	2(5)	100-200			
1978/03/26	30	5.6	260	6	6	76-316			
1980/06/25	0.3	-	152	3	3	155-310			
1982/12/25	1.7	4.8	112	4	4	90-190			
1984/10/18	1.4	4.5	106	5	5	35-160			
1968/07/12		5.3	172	2		80-90			
1968/12/18		5.0	194	3		200-510			
1970/06/28		5.7	332	2		200-240			
1980/09/25		4.77		3		100-160			
1971/12/15		4.9	115				9		7.5-85
1987/05/06							9		13-83
1987/12/20							9		13-83
1988/10/18							9		11-77
1989/02/17							9		10-77

pile570 effective stress simulation. Almost all of the historic granite data, and the Degelen data received to date, lie on or below this prediction. The four shaded triangles in the left plot of Figure 5 are the peak velocities from the records shown in Figure 1, all from gauges emplaced at the Piledriver source depth of burial. The two gauges at larger ranges, that give relatively lower peak velocities, and most of the other gauges emplaced at depths above the explosion working point, were located on the opposite side of the source from the two closer-in gauges.

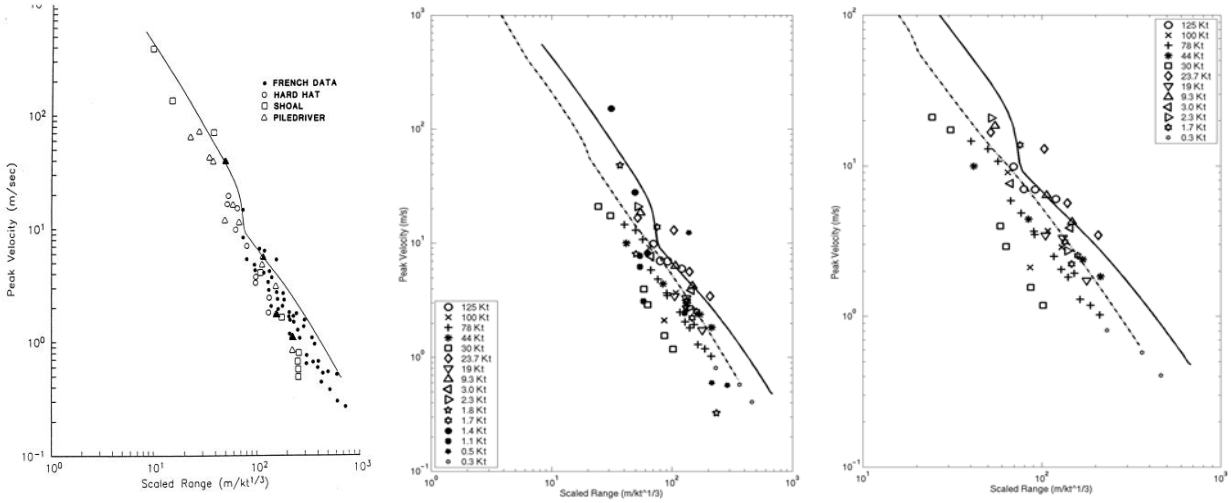

Figure 5. Peak particle velocity vs. scaled range for historic data from US and French explosions (left), for the 16 Degelen explosions digitized to date (center), and for the 12 Degelen events designated as showing free-field pulse shapes (right). The solid line is the prediction from the pile570 effective stress simulation shown earlier in Figure 1. The dashed line is the predicted peak velocity for the Degelen DE12 simulation.

The very first sets of digitized data received from IDG (plotted in Rimer, *et al*, 1999) did not include the Degelen explosions with relatively high peak velocities. Thus, these early Degelen peak velocities appeared at that time to be near the lower bound of the historic granite data. A Degelen simulation model, consisting of the Sammis failure model, followed by a large reduction in frictional strength for rubbleized rock elements, was developed to match the pulse widths from the first sets of digitized Degelen data. This model, labeled as DE12 in Rimer, el al (1999), is shown as a dashed curve in the two right plots of Figure 5. It provides a better fit on average to all of the Degelen particle velocity peaks than does the higher peak velocity pile570 simulation. However, this DE12 model, as will be shown below, is consistent with only a subset of the Degelen data received more recently from IDG.

We have carefully analyzed the near-field particle velocity pulses from the first 16 Degelen explosions of Table 1 and excluded the data from four of these events as more characteristic of localized fault or block motions than of free-field ground motion. Pulse widths from three of the four events in general show very wide positive velocity pulses with almost constant outward velocity plateaus extending from some point after peak velocity to the end of the digitized data. These excluded events have explosive yields of 1.1, 1.8, and 1.4 kT. The fourth event, having a yield of 0.5 kT, has two records that look like the block motions from the first three excluded events, and two at larger scaled ranges with very large positive pulses that do have more of a free-field shape, but have almost no negative velocities. Another event, with explosive yield of 0.3 kT, is borderline, with reasonable pulse shapes obtained at scaled ranges larger than any of the other Degelen data. These records, however, have scaled positive and negative pulse widths much larger than the rest of the data. We have included this event in the free-field data set shown on the right plot (with the enlarged scale) in Figure 5. This 12 event "free-field set" thus consists of the 8 explosions with yields greater than 9 kT and only 4 events with lower yields (3 kT or less). It is not surprising that a significant fraction of the data from the lower yield, and thus shorter wave length, explosions appear to be more contaminated by local block motion. This free-field set, apart from the data from the high velocity 23.7 kT explosion, and the very low velocity 30-kT explosion, shows considerably less scatter about the dashed DE12 prediction than did the full data set.

To more easily compare the individual Degelen "free-field" particle velocity pulses from explosions of different yields, we have cube-root-of-yield-scaled these data to the Piledriver yield of 62 kT. Since the quality of the particle velocity pulse data vary greatly between explosions and even between records from the same explosion, we reduced the data to be plotted from 56 particle velocity pulses to a somewhat more manageable best quality 34. These were further subdivided into a subset of 24 records from 8 explosions that have relatively wide positive pulses (shown in Figures 6) and a smaller subset of 10 records from 3 explosions that have narrower positive pulses (shown in Figure 7). In each Figure, the records have been ordered by increasing scaled range and have been plotted together with results at the same range from the DE12 simulation. Almost all of the omitted 18 records were from the larger wide pulse subset. Since the original digitized data did not contain the actual explosion zero times, the data in each plot has been time-shifted to correspond roughly to the arrival times of the numerical simulation. In the following discussions, individual particle velocity records will always be referenced by their scaled to 62-kT ranges and original explosive yields.

The DE12 model was designed to simulate the pulse widths from the first two explosions listed in Table 1 (2.3 and 19 kT) as well as a few of the records from the third (78-kT) explosion. All three of these free-field explosions were later categorized as belonging to the wide pulse subset. This simulation was also required to give a cavity radius and a Reduced Displacement Potential (RDP) consistent with general observations from the Degelen site. Agreement between simulated and measured positive and negative pulses was best at the 704 m range from the 19-kT explosion, but the measured positive pulse at the 741 m range (and other ranges) from the 78-kT explosion are somewhat narrower than those simulated. Only two partial records are available from the 2.3-kT explosion, with one of these, at 551 m, considerably wider than other explosion records at similar scaled ranges. As more digitized data were received from the 78-kT event, and still later from the other events of the data set, it became clear that there is a significant gradation of pulse widths within even the wide pulse subset.

Some of the wide pulse data exhibit a second positive pulse with either a second obvious peak or traces of a plateau similar to both the DE12 simulation and the data at 704 m from the 19-kT explosion, while others show no evidence of such a second pulse. As an example, for the 1.7-kT event, all four of the records shown in Figure 6 appear to give consistent shapes that include such a second pulse. The gauges from the closest-in and furthest-out of the four ranges, located near the emplacement tunnel, give positive pulse widths in good agreement with DE12, while the middle two gauges, at substantially different azimuths from the others, give narrower pulses. In contrast to these

data from the 1.7-kT event, most of the records from the 78-kT and 44-kT explosions exhibit little or no second pulse.

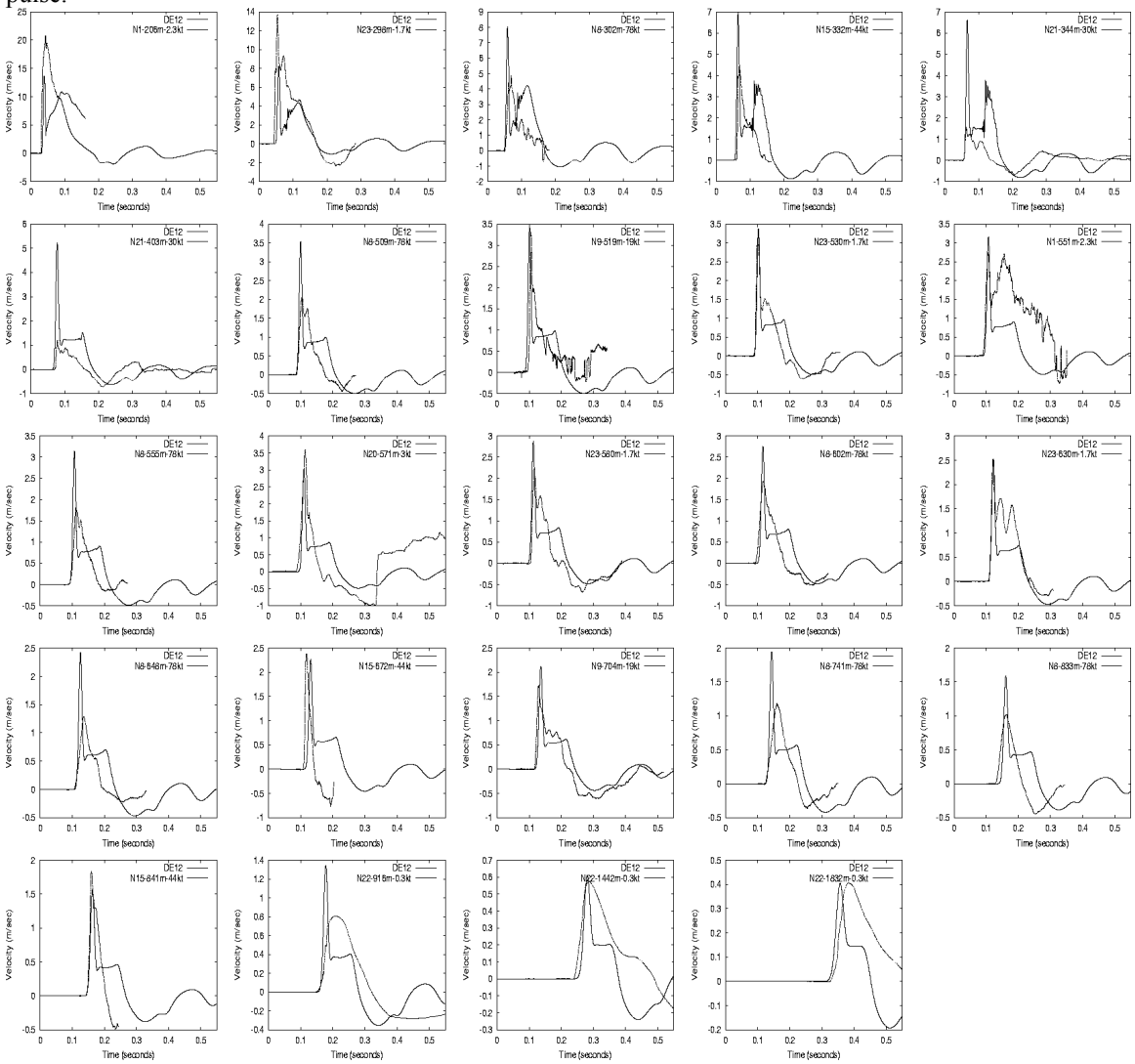

Figure 6. Particle velocity pulses (scaled to Piledriver yield) from the "wide pulse" Degelen data subset compared with the results of simulation DE12 (the solid curves).

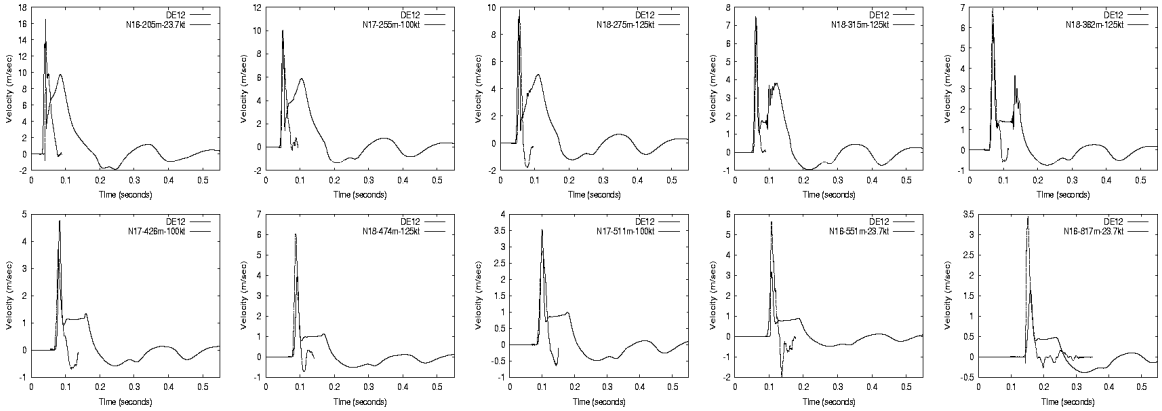

Figure 7. Particle velocity pulses from the "narrow pulse" data subset compared with the results of DE12.

It is of course possible that some or all of the recorded second pulses are either the result of some systematic errors in gauge response or perhaps indications of some non-free-field response of the rock at these sites. In the absence of convincing evidence, we are choosing to treat these records as free-field. This leads to the hypotheses that the material models required to simulate the records from even just the wide pulse subset, or more likely the material constants within any one particular set of material models, may be different for each explosion site.

The particle velocity records from the three "narrow pulse" explosions shown in Figure 7 give somewhat different peak amplitudes, but very similar positive pulse shapes. In general, these records do not exhibit the two pulse structure apparent in much of the wide pulse subset. The majority of these plots also show narrow negative pulses, although at least one record from each of the three explosions does not show such a negative.

With one exception, every positive pulse shown from the 8 explosions in Figure 6 is much wider than any of the pulses from the three explosion "narrow pulse" subset shown in Figure 7. This exception is the 44- (or 18-) kT explosion that does not fit very well in either the wide or narrow subsets. The 44-kT explosion has one wide pulse, at the smaller range of 332 m, one narrow pulse, at the middle range of 672 m, and a pulse slightly narrower than the wide pulse subset at the larger range of 841 m. We have chosen to place this explosion in the wide subset for two reasons. First, the narrow pulse explosions of Figure 7 also tend to show very narrow negative pulses, while the most complete negative pulse record from the 44-kT event, at 672 m, is wider than those of Figure 7. Second, if we use the smaller of the two explosive yields given to us for this event, and scale up to 62 kT, positive and negative pulse widths increase by about 35 percent from those shown in Figure 6.

The two very low amplitude records from the 30-kT explosion that are shown in Figure 6 (and those at smaller ranges that are not shown) have pulse shapes and pulse widths similar to others of the wide pulse subset. In the absence of specific site material properties for this and other explosion sites, we have no satisfactory explanation for the low peak amplitudes from this explosion. Depth of burial is consistent with those for the other large explosions of Table 1 that were at sites described as in granite. Only the narrow pulse 100- and 125-kT explosions, at sites described as in quartz porphoryte, were more deeply buried. The m_b values given in Table 1 also do not provide any confirmation of the low near-field particle velocity amplitudes from the 30-kT event.

Figure 8 shows comparisons between records at three of the four ranges shown earlier from Piledriver (the solid curves) and some of the records from similar scaled ranges from wide pulse Degelen explosions, scaled to 62 kT. Representative records from the wide pulse Degelen explosions are not available at scaled ranges approximating the 207 m range of the first (and widest) Piledriver particle velocity record. Near the 470 m range, the Piledriver positive and negative pulses are clearly much wider than those from Degelen explosions, although the general shapes of the Piledriver and Degelen positive pulses are quite similar.

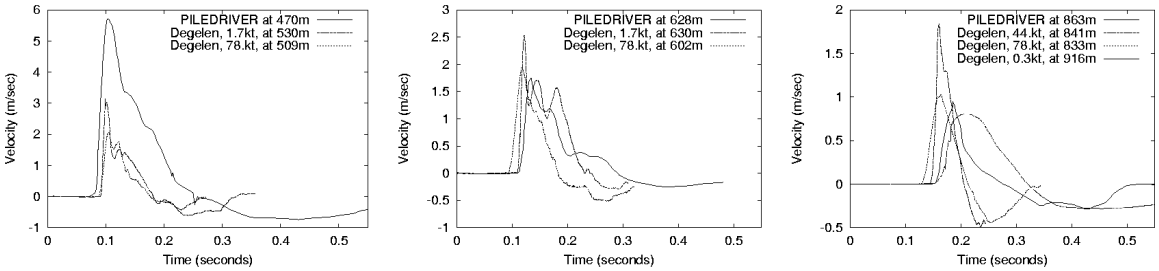

Figure 8. Comparisons between particle velocity pulses at three ranges from Piledriver and from Degelen wide pulse explosion records (scaled to 62 kT) at nearby scaled ranges.

Differences between the records from the US and Degelen granite sites are less obvious at the two larger ranges. We have seen earlier that the peak amplitudes from Piledriver are small at these two ranges relative to those that would be predicted from the two closer-in records. At 628 m, the Piledriver record looks very similar to the record from the 78-kT event out to a time of roughly 0.2 seconds (if the arrival time of the 78-kT record is shifted to coincide with the Piledriver arrival). Near 0.2 seconds, the Piledriver positive pulse at 628 m begins to stretch out in time, with an almost constant velocity plateau visible on this record, giving a much later time zero crossing and a wider negative pulse than both the Degelen records. At this range, the record from the 1.7-kT explosion shows a steeper rise to peak, multiple peaks, and a significantly wider positive pulse than the Piledriver record, at least until

that record begins to stretch out in time. The Piledriver record at 863 m also shows such a stretching, but not the constant velocity plateau recorded at 628 m. The record from the 78-kT event is in good agreement until this stretching begins.

The particle velocity comparisons made near the 863 m range illustrate the large gradation in pulse shapes and pulse widths recorded from Degelen "wide pulse" explosions, with the 44-kT record showing a steeper rise, a higher peak, a narrower pulse, than the 78-kT record, but a similar negative peak. The narrowest of the three very wide pulses obtained from the scaled 0.3-kT explosion is wider than the Piledriver record at a slightly smaller scaled range. When these particle velocity records are time-integrated, only the Piledriver records at the two closest-in ranges (207 and 470 m) give peak displacements significantly larger than all of the Degelen records at comparable scaled ranges. Peak displacement from the 1.7-kT explosion is similar in magnitude to that from Piledriver near 628 m.

We next examine the digitized near regional seismic records. The 8 explosions with digitized seismic data include all 3 of the narrow pulse subset. The primary purpose of this analysis of the 8 largest Degelen explosions for which we have such data is to determine whether or not the differences in pulse widths observed for the near-field data are observable at larger, seismic ranges. Based on the near-field observations, we would expect the seismograms at larger ranges from the "narrow pulse" subset of explosions to have relatively smaller amplitudes.

We first empirically determine a distance correction for the 8 explosions. We determine a slope of log(Amplitude) vs. distance for each event, and then find the average of the slopes, weighted by the number of points contributing to each curve. The distance correction is approximately -.014 of log(amplitude) in mm per km. The data for each explosion is then corrected to a 10 km distance. Assuming $\log_{10}(\text{amplitude})=B\cdot\log_{10}(\text{yield})+C$, these data are used to estimate a B of 0.76 and a C of -1.76. These values do not change significantly if we determine them separately from the narrow and wide pulse data subsets. From just the wide pulse data we obtain B=0.83 and C=-1.8, and from the narrow pulse data we obtain B=0.79 and C=-1.7. Figure 9 shows log amplitude versus distance, corrected for distance and yield using the values of B and C above obtained for all the seismic data. Figure 10 shows the mean values for each event, of the data in Figure 9. There is no apparent difference in near regional amplitude between the explosions with narrow and those with wide velocity pulses in the near field.

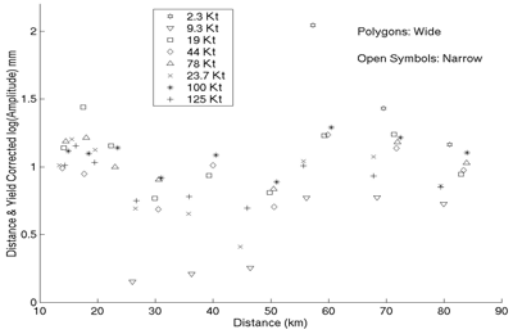

Figure 9. Distance and yield corrected log amplitudes of vertical seismograms recorded from 13 to 84 km. Open symbols (+, *, and x) are used for events that have narrow velocity pulses in the near field, and polygons are used for events that have wide pulses.

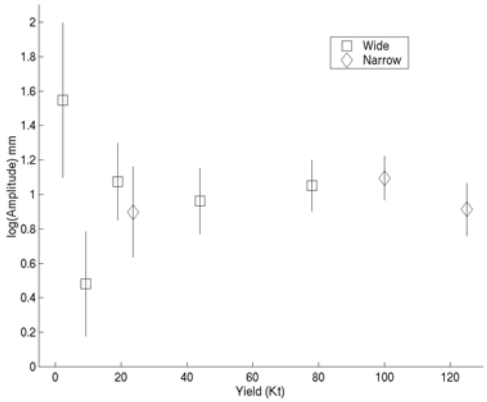

Figure 10. Mean values with one standard deviation confidence intervals for each event for the data shown in Figure 9.

Numerical Modeling of Explosions

The near and far field data from US and Degelen explosions have provided a set of constraints to test out several competing mechanisms for both the "failure/rubblization process" and the post-failure "strength reduction" process. The 3 strength reduction mechanisms and 2 rock failure mechanisms given in Table 2 have been emphasized, first for Piledriver, and then for the wide pulse Degelen events. Here, Yield/Failure (YF) refers to a model in which the yield and failure surfaces coincide, a no bulking flow rule, and a failure surface based on laboratory tests on fractured granite. Finite plastic work is required for rubblization and a standard friction law used for rubblized rock. In the Shock Damage (SS) model, strength reduction to a damaged friction law failure surface is based on the shear strain in the element, mimicking the lateral stretching of a rock element during the divergent outward motion. Parameter studies have been completed using both competing failure/rubblization processes together with each of

the strength reduction mechanisms that are appropriate. (Pore pressure buildup in the effective stress process is incompatible with the crack opening in the Sammis model.) Reasonable simulations of the Piledriver data (particle velocities, cavity radius, RDP) have been obtained for each combination denoted by the letter P in Table 2.

Table 2. **Combinations of failure/rubblization processes and strength reduction mechanisms for which simulations of Piledriver (P) and Degelen wide pulse explosions (D) have been accomplished.**

Strength Reduction Mechanisms/ Failure/Rubblization Processes	Shock Damage (SS)	Acoustic Fluidization (AF)	Effective Stress (EF)
Sammis Damage Mechanics (SA)	P, D	P, D	
Yield/Failure (YF)	P, D	P, D	P

Our goal was to use parametric simulations of the near and far field data from Degelen events to further evaluate and perhaps discriminate between these competing physical mechanisms. Our preliminary calculations of the 3 narrow pulse explosions to date show that the best fits to both the positive and negative pulses are obtained using the YF model and no strength reduction model. This best fit to date of the narrow pulse velocity data also gives a cavity radius of 29.0 m, just within the 28-36 m range of the Degelen observations. A static RDP of about 6,000 m^3 and a peak RDP of roughly 7500 m^3 were computed from this simulation. This computed peak RDP was only slightly larger than the peak RDPs that were obtained from the particle velocity data from narrow pulse explosions. All Degelen calculations were made using an overburden pressure of 50 bars, much smaller than the 120 bars for the deeper Piledriver event. Use of the larger overburden pressures consistent with the 35–75% larger depths of burial of the narrow pulse explosions would be expected to reduce the amplitudes of the simulated RDPs somewhat.

The parametric calculations made to date for the 9 wide pulse explosions indicate that each of the 4 model combinations in Table 2 can be made to fit some of the features of the Degelen data. We have ordered the best simulations with each of the four model combinations from best overall fit to worst fit as follows: 1) SA-SS, 2) YF-AF, 3) SA-AF, 4) YF-SS. Note that we have had more extensive experience with the effects of parametric changes in the SA-SS models dating back to Rimer, *et al* (1999) and the DE12 simulation. However, our best efforts so far have not resulted in simulations using the other model combinations that provide as good a fit to as many (but certainly not all) of the wide pulse records as did the SA-SS combination. Figure 11 shows comparisons between the simulated and measured particle velocity pulses from the SA-SS best fit. Note that in comparison with the DE12 results shown earlier in Figure 6, the peak velocities are smaller, and positive pulses are narrower, thus greatly increasing the quality of the match to much of the Degelen wide pulse data set. This was accomplished by a single, but significant, change in the DE12 parameter set (Table 6-1 of Rimer, *et al*, 1999), i.e., reduction of the slope in the linear shear modulus reduction vs. damage parameter relation from 400 to 300 kb. This parameter change results in less reduction in shear and bulk moduli near the cavity, less dilatant behavior near the cavity, less P-wave velocity reduction near the cavity, and thus a weaker (narrower), dilatant, second positive pulse, a smaller static RDP of 11,000 m^3, and about a 10% larger final cavity radius (34.5 m).

The model combinations made using an improved version of the acoustic fluidization model provide best fits that are clearly superior to the best fit we could get so far using the YF-SS model. This version incorporates the "block model" described in Melosh and Ivanov (1999) which represents the motion of a system of oscillating blocks as a viscous motion with an effective kinematic viscosity whenever shear stress is larger than the Bingham limit. This shear stress dependence replaces the dependence of the frictional strength upon kinetic energy in our earlier implementations of AF.

CONCLUSIONS AND RECOMMENDATIONS

IDG is in the process of digitizing data from 25 nuclear tests at the Degelen test site. The complete data set consists of 81 near field waveforms recorded underground at shot depth and 124 (unique) near regional seismic records. IDG has digitized 75 near field waveforms and 97 seismic waveforms (including multiple records of the same signal), and will complete digitization of the remainder over the duration of this project. The data set of near field and regional waveforms will be delivered to the Center for Monitoring Research upon completion of this project.

We are in the process of modeling this data. The goal is to develop material models that are consistent with the data and have a realistic physical basis. Work to date has focused on implementation and testing of improved numerical

modeling procedures and simulation of near regional data. We are testing acoustic fluidization as a physical mechanism for strength reduction in nonlinear explosion simulations. Preliminary results are promising, but additional work is required to improve the realism of the models. During the next year, we will continue this modeling effort. Near field data will be modeled with our nonlinear finite difference code as described in this report. Near regional data will be modeled using wave number integration. We plan to also look at observed teleseismic amplitudes from explosions with wide and narrow near field velocity pulses to see whether these correlate.

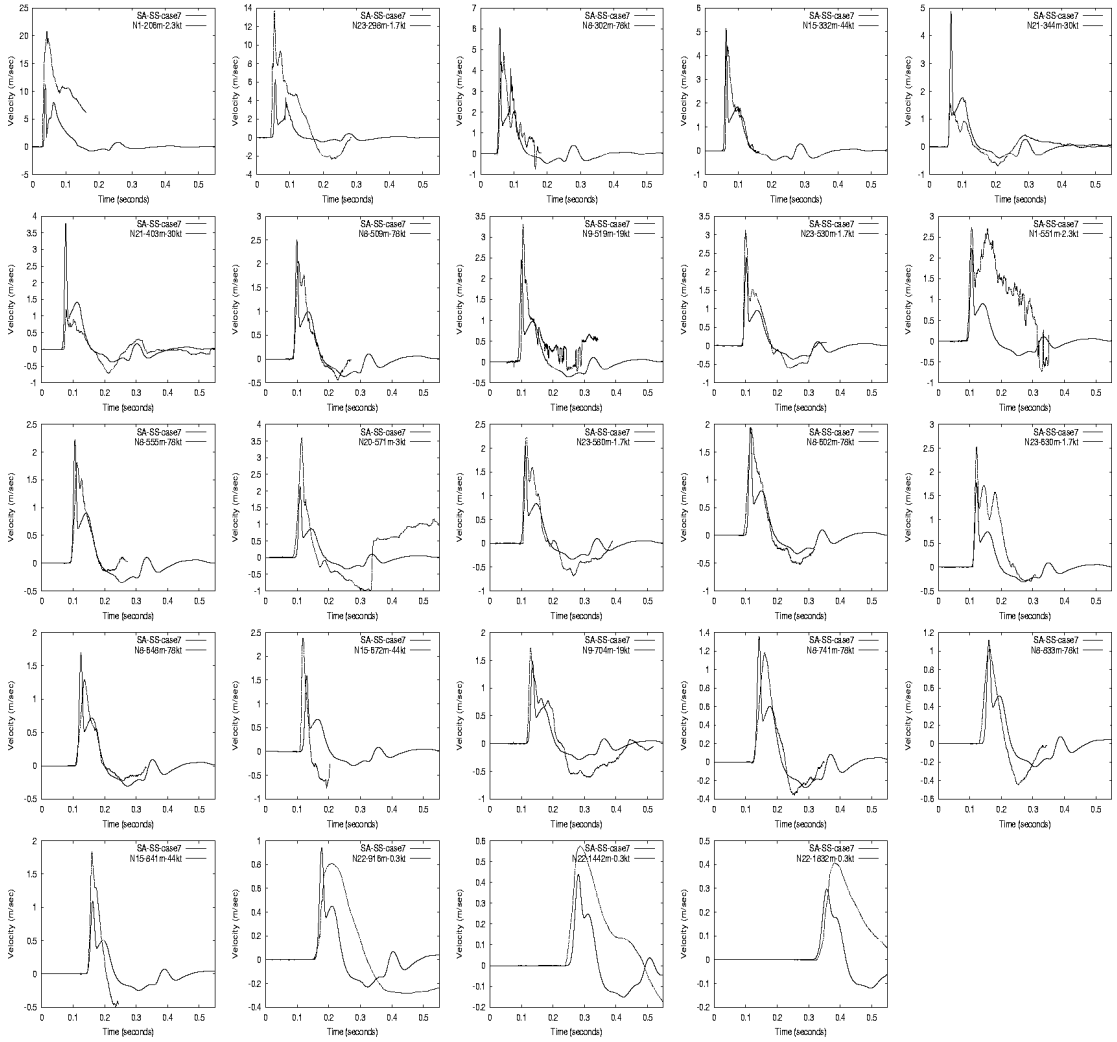

Figure 11. Comparison between particle velocity pulses from the wide pulse Degelen subset and the results of the best fit simulation using the SA-SS model combination (the solid curves).

REFERENCES

Melosh, H.J. (1979), "Acoustic Fluidization: A New Geologic Process?," *J. Geophys. Res*., **84**, 7513, December.

Melosh, H.J., and B.A. Ivanov (1999), "Impact Crater Collapse," *Annual Rev. Earth Planet Science*, **27**, pp385-415.

Rimer, N., S. M. Day, G. A. Hegemier, H. E. Read, S. K. Garg, and S. Peyton (1984), "Effect of Pore Fluid Pressure on Explosive Ground Motions in Low Porosity Brittle Rocks," DNA-TR-85-245, July.

Rimer, N., J.L. Stevens, J.R. Murphy, and G.G. Kocharyan (1999), "Estimating Seismic Source Characteristics of Explosions in Hardrock Using a Micro-Mechanical Damage Model," Maxwell Technologies Final Report MTSD-DTR-99-16423, July.

Stevens, J. L., N. Rimer, and S. M. Day (1986), "Constraints on modeling of underground explosions in granite," S-CUBED annual report, AFGL-TR-86-0264, SSS-R-87-8312, October.